# Determination of the draft force for different subsoiler points using discrete element method

Li Bo, Xia Rui, Liu Fanyi, Chen Jun*, Han Wenting, Han Bing

(*College of Mechanical and Electronic Engineering, Northwest A&F University, Yangling, 712100, China*)

**Abstract:** Generally, a subsoiler is comprised of a shank and a point. The point shape has a significant effect on the draft force of a subsoiler. In this study, the draft force of subsoilers with four different points were compared under the speed of 0.8 m/s and the depth of 350 mm in the soil bin. Discrete Element Method (DEM) was applied in simulating the working process of the subsoiler. The stiffness of soil particles used in DEM was calibrated by comparing the simulated draft force of a standard arc-shaped subsoiler with the experiment. The calibrated soil particle stiffness was $1.1\times10^4$ N/m. The validated model was then used to compare the draft force of subsoilers with four different points under the same condition in the test. Results showed that different points would cause different draft forces. The subsoiler with short chisel point caused the smallest draft force (2885 N) while the point with short face and wings had the largest force (4474 N). The relative errors of the simulated results were less than 4%, which proved that DEM was an effective way for predicting the draft force of subsilers. The velocity field and contact force filed could show the movement of soil around the subsoiler.

**Keywords:** subsoiler, point shape, draft force, chisel point, DEM, conservation tillage

**DOI:** 10.3965/j.ijabe.20160903.2210

**Citation:** Li B, Xia R, Liu F Y, Chen J, Han W T, Han B. Determination of the draft force for different subsoiler points using discrete element method. Int J Agric & Biol Eng, 2016; 9(3): 81－87.

## 1 Introduction

Tillage can improve the soil condition and structure, which has a great influence on production increase. As a part of conservation tillage, subsoiling helps to reduce soil degradation and erosion, which is beneficial for sustainable development[1-3]. Moreover, subsoiling also saves energy considerably compared with traditional tillage patterns. Subsoilers could also be used for breaking down the impermeable horizon of meadow soil[4] which was a poor yield soil. Subsoilers have become the most important tillage tool for farming around the world. However, too large draft force is the most serious existing problem of subsoilers which hindered their future promotion.

The subsoiler's geometry contributes greatly to the draft force and tillage performance. Researchers have designed different shapes of subsoilers to reduce the draft force and increase the soil disturbance. There are mainly two types of shank, including the curved and the linear one. Different points of subsoiler have been designed and some of them have wings. Researchers have found that points' shape has a great influence on tillage performance[5]. Subsoilers with wings were designed to enhance the disturbed area, however, the draft force would also increase. Luo et al.[6] compared the chisel-shape subsoiler with the double winged subsoiler and found that subsoiling could enhance crop yield enormously and the double winged subsoiler had a better

**Received date:** 2015-10-28 **Accepted date:** 2016-04-28

**Biographies: Li Bo,** PhD candidate, research focuses on agricultural engineering, Email: nwsuaf_lb@126.com; **Xia Rui,** Master, research focuses on mechanical engineering, Email: 648509152@qq.com; **Liu Fanyi,** PhD candidate, research focuses on agricultural engineering, Email:1017856727@qq.com; **Han Wenting,** PhD, Professor, research focuses on agricultural electrification and automation, Email: hanwt2000@126.com; **Han Bing,** Master, Advanced experimenter, research focuses on agricultural engineering, Email: hanbing0506@nwsuaf.edu.cn.

***Corresponding author: Chen Jun,** PhD, Professor, Northwest A&F University, No. 22, Xinong Road, Yangling, Shaanxi 712100, China. Tel: 029-87091867, Email: chenjun_jdxy@nwsuaf.edu.cn.

performance. Ahmed and Godwin[7] found that the longitudinal position of subsoiler wings did not significantly influence the draft force or the disturbed area. Oni et al.[8] tested twenty-nine model tools and found that the nose angle and working depth have significant effects on draft force. Shmulevich et al.[9] compared the soil resistance of four cutting blades by simulation, which were well matched with tests. Theoretical methods have been utilized to study the interaction between soil and tillage tools[10,11]. Traditionally, experiments are needed as a subsoiler newly designed, which is time consuming and heavy labor work is required. To simplify the process of optimizing the structure of subsoilers, computer-aided design program and simulation methods have been applied as an accurate and effective way[12].

Numerical models such as finite element methods (FEM) were used for modeling soil-tool interaction[13]. Many researchers have tested the effect of point on draft force and tillage quality using FEM. Mouazen compared four subsoilers geometrical types using FEM and found that the subsoiler having a shank of 75° rake angle and a chisel of 15° recorded the smallest draft force. The results were validated by soil bin tests[14,15]. Mouazen[16] studied the effects of soil moisture, bulk density and working depth on draft force of subsoilers using FEM. The simulation results were validated by the test. However, FEM could not simulate the displacement of soil particles and crack propagation during the working process. DEM is a method mainly dealing with discontinuous particles, which has been used to simulate soil-tool interactions by many researchers[17-19]. Zhang et al.[20] simulated the working process of a bionic bulldozing plate using DEM and obtained reasonable results after comparing the simulation results with soil bin tests. Chen et al.[21] calibrated the discrete element model of three different soils by comparing the draft and vertical force with the experimental data. The model could be used for predicting soil disturbance characteristics. The application of DEM in analyzing soil-tool interactions has been summarized by Shmulevich[22]. A DEM software, PFC$^{3D}$[23] was utilized in this study to establish the soil-subsoiler interaction model. The particle stiffness was calibrated by comparing the simulated draft force of an arc-shaped subsoiler with the soil bin test. The calibrated model was then used to simulate the working process of subsoilers with four different points. The simulation results were validated by the soil bin test. The objectives of this study were to (1) establish the soil-subsoiler interaction model using DEM (2) investigate the impacts of four points' shape on subsoiler's draft force.

## 2 Methodology

### 2.1 Model subsoilers

To compare the draft force of four different points, the same shank was used. These four points as well as the shank are shown in Figure 1 and the geometrical parameters of them are shown in Table 1.

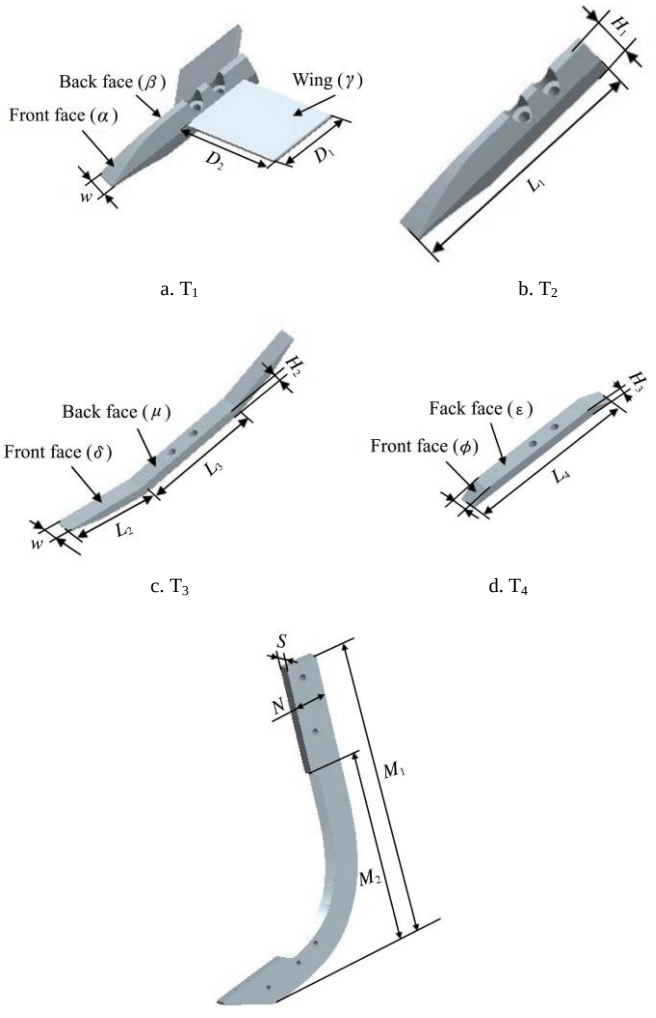


Figure 1 Four different points and the shank

**Table 1 Geometrical parameters of four points and shank**

| Symbol and unit | Value | Symbol and unit | Value |
|---|---|---|---|
| $\alpha$ /(°) | 50 | $L_3$ /m | 0.175 |
| $\beta$ /(°) | 30 | $H_2$ /m | 0.013 |
| $\gamma$ /(°) | 75 | ø/(°) | 55 |
| $w$ /m | 0.030 | $\varepsilon$ /(°) | 30 |
| $D_1$ /m | 0.104 | $H_3$ /m | 0.014 |
| $D_2$ /m | 0.135 | $L_4$ /m | 0.253 |
| $H_1$ /m | 0.054 | $s$ /m | 0.030 |
| $L_1$ /m | 0.257 | $M_1$ /m | 0.780 |
| $\delta$ /(°) | 18 | $M_2$ /m | 0.500 |
| $\mu$ /(°) | 30 | $N$ /m | 0.09 |
| $L_2$ /m | 0.125 | | |

These four points are: $T_1$ - short face with wings, $T_2$ - short face without wings, $T_3$ - chisel type with the long edge, $T_4$ - chisel type with the short edge. The shank is a curved one which is widely used for tillage. The $T_1$ and $T_2$ were in the same shape except a pair of wings. For the shank that was mounted on the traction wagon 75 ° from the horizontal line during the working stage, the values shown in Table 1 were measured when the subsoiler was mounted on the traction wagon.

## 2.2 Development of soil-subsoiler interaction model

### 2.2.1 Soil domain

The soil domain was 1.5 m long, 1.2 m wide, and 0.5 m high. The soil bin was established 0.3 m higher than the soil domain to keep all soil particles inside (Figure 2). Considering the calculating time of the computer, soil particle diameter was set to 20 mm which was much larger than the real particle. The total number of soil particles in the soil domain was 136 612. The parallel bond model (PBM) was applied for generating bonds which represent cohesion between soil particles. Parameters used for imputing were particle normal stiffness: $K_n$ (N/m), particle shear stiffness: $K_s$ (N/m), particle friction coefficient: $\mu$ (dimensionless), bond normal stiffness: $\overline{K_n}$ (Pa/m), bond shear stiffness: $\overline{K_s}$ (Pa/m), bond normal strength: $\bar{\sigma}$ (Pa), bond shear strength: $\bar{\tau}$ (Pa), bond radius multiplier: $\overline{R_m}$ (dimensionless), local damping coefficient ($\theta$), and viscous damping coefficient ($\omega$). The values of soil parameters of particles used for this study were taken from previous studies[24,25] for a sandy loam soil except for $K_n$. The $K_s$ was assumed to be the same as $K_n$ according to Van der Linde[26]. Thus only the particle normal stiffness needs to be calibrated. The stiffness of the subsoiler was assumed to be the stiffness of steel: $1\times10^9$ N/m.

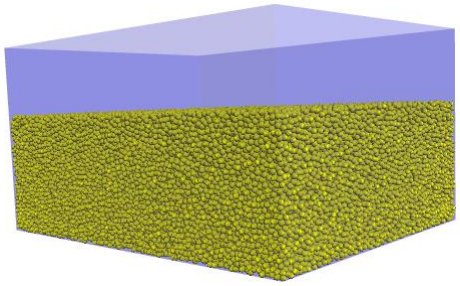

Figure 2 Model of soil domain

**Table 2 Parameters used for modeling**

| Parameter | Description and unit | Value |
|---|---|---|
| $K_n$, $K_s$ | Particle normal and shear stiffness /N m$^{-1}$ | To be calibrated |
| $\mu$ | Particle friction | 0.5 |
| $\overline{R_m}$ | Radius multiplier | 1 |
| $\overline{K_n}$ , $\overline{K_s}$ | Normal and shear bond stiffness /Pa m$^{-1}$ | $4\times10^5$ |
| $\bar{\sigma}$ , $\bar{\tau}$ | Normal and shear bond strengths /Pa | $2\times10^4$ |
| $\theta$ | Viscous damping coefficient | 0.5 |
| $\omega$ | Local damping coefficient | 0.7 |

### 2.2.2 Calibration

Particle stiffness was calibrated by comparing the simulated draft force of a standard arc-shaped subsoiler traveling through the soil bin with the test data. The dimensions of the arc-shaped subsoiler (Figure 3b) were based on JB/T 9788-1999[27]. The shank was positioned vertically as it traveled both in the simulation (Figure 3a) and experiment according to its working requirement.

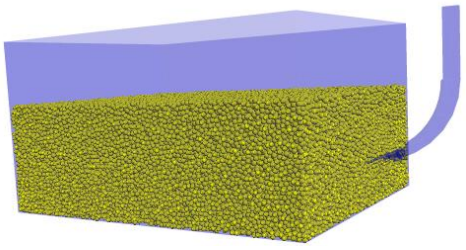

a. Soil-subsoiler interaction model

b. The arc-shaped subsoiler

Figure 3 Calibration using a standard arc-shaped subsoiler

The arc-shaped subsoiler was simulated under the speed of 0.8 m/s and depth of 300 mm which was the maximum working depth for this subsoiler. For calibration, the simulation used a group of assumed values of $K_n$ and compared them with the test results to investigate the best matched value of $K_n$. The test of this arc-shaped subsoiler was done using the same instruments with others subsoilers tested in this study and the test condition was the same with the simulation.

### 2.3 Comparison of four subsoilers using DEM

The model of the subsoiler was constructed and saved as the STL format which could be imported into PFC$^{3D}$. STL is a format that models a tool using triangle elements which could reflect the real tool accurately and save calculating time.

An example of a subsoiler- $T_1$ is shown in Figure 4. In the initial state, different points were mounted onto the subsoiler positioned at the end of the soil bin at a constant depth of 350 mm. The shank's angle of inclination was 75 º from the horizontal line. The virtual subsoiler traveled through the soil bin at a constant speed of 0.8 m/s. These four subsoilers traveled at the same speed and depth for comparing the impact of point's shape on draft force. The draft force was monitored by PFC$^{3D}$ during the working process of each subsoiler.

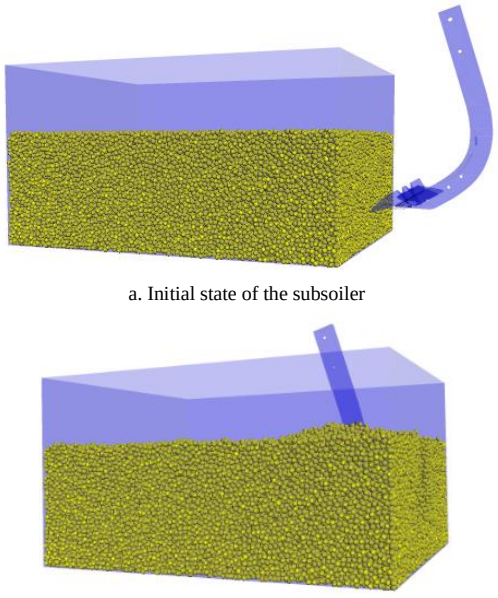

a. Initial state of the subsoiler

b. Working state of the subsoiler

Figure 4 Model of subsoiler-T1 interacting with soil

### 2.4 Experiment

#### 2.4.1 Soil preparation

To validate the simulation results, soil bin test was done in the agriculture machinery lab, Northwest A&F University, Yangling, Shaanxi, China. Sandy loam soil was used for the test. Before doing the experiment, the soil needed to be prepared including tillage, breaking clods, watering, leveling and compacting by a roller. The moisture content of the prepared soil was 19% (weight percentage), and the rigidity of the soil at depth of 350 mm was 500-600 kPa for this test. The bulk density of the soil was 1656 kg/m$^3$, and the porosity of the soil was 0.4.

#### 2.4.2 Instruments and measurement

Draft force of four subsoilers were compared in this study by the instruments shown in Figure 5. The shank was mounted on the frame 75 º from the horizontal line. The driving force provided by the traction wagon could drag the subsoiler working at a stable speed (0.8 m/s) and specified depth (350 mm). Sensors, including the upper link sensor (CYB-602S, measuring range: 0-10 kN) and the hanging pin sensor (CYB-601S, measuring range: 0-15 kN), could measure the draft force of subsoilers timely. These three sensors were mounted on the three point linkage of the traction wagon.


1. Subsoiler 2. Frame 3. Depth wheel 4. Right hanging pin sensor of CYB-601S 5. Left hanging pin sensor of CYB-601S 6. Upper link sensor of CYB-602S 7. Traction wagon

Figure 5 Instruments used in the test

The working principle of data collecting system in the experiment is shown in Figure 6. The upper link sensor, hanging pin sensor and angle sensor transferred the measured data to the dynamic data collector. Built in the upper link sensor, the angle sensor was used for the calculation of horizontal forces measured by the upper link sensor. The draft force is the horizontal vector

sum of these forces. The data collector sends the data through the antenna to a laptop which will finally deal with the data. The data sample rate was 5 Hz for this measurement.

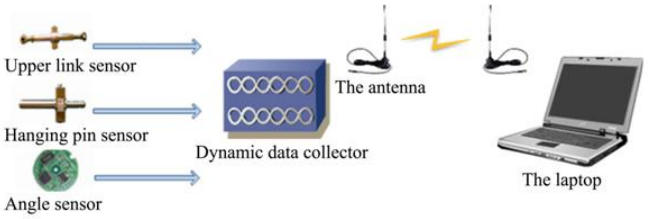


Figure 6 Working principle of data collecting system

## 3 Results and discussion

### 3.1 Calibrated results

The measured draft force of the arc-shaped subsoiler in the test was 2021 N. Meanwhile, it was simulated by PFC$^{3D}$ using a group of assumed values of $K_n$. The relative errors were calculated by comparing the simulated force with the test data (Table 3). The simulated draft force increased from 1943 N to 2195 N as $K_n$ increased from $9.0\times10^3$ N/m to $1.3\times10^4$ N/m. The relative error was minimum when $K_n$ equaled $1.1\times10^4$ N/m. Therefore, the particle stiffness of $1.1\times10^4$ N/m was used for the simulation of our subsoilers.

**Table 3 Calibration by adjusting the particle stiffness ($K_n$)**

| Assumed $K_n$/N m$^{-1}$ | Simulated draft force/N | Relative error/% |
|---|---|---|
| $9.0\times10^3$ | 1943 | 3.86 |
| $1.0\times10^4$ | 1962 | 2.92 |
| $1.1\times10^4$ | 2063 | 2.08 |
| $1.2\times10^4$ | 2107 | 4.26 |
| $1.3\times10^4$ | 2195 | 8.61 |

### 3.2 Draft force

The draft forces of four subsoilers versus travel distance were recorded in Figure 7. For all the four curves, the draft force increased gradually as the subsoiler entered the soil bin. Then the draft force reached a stable state as the subsoiler entered into the soil domain completely. The average force taken from the stable section from 0.7 m to 1.4 m was considered as the simulated draft force of the four subsoilers. The draft force of $T_1$ was the biggest among all the four points because of the wings which contributed to the largest soil disturbance. Other three curves were closed to each other, however, it still could be observed that $T_4$ was the smallest force.

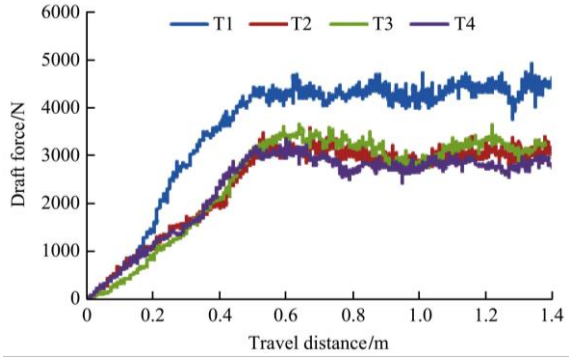


Figure 7 Simulated draft force

The draft forces of four subsoilers in the stable section are shown in Figure 8. All curves were fluctuated around their average value. The draft force of $T_1$ was much higher than other three, the same trend was shown in Figure 7. The force in the soil bin test had greater volatility than that in the simulation, which was caused by the inhomogeneity of soil conditions and the size of clods in the soil bin.

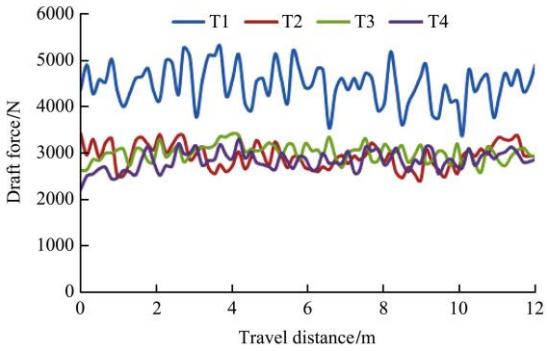


Figure 8 Tested draft force

Relative error was used to validate the accuracy of the simulations. The relative error was calculated as follows.

$$RE = \frac{|F_s - F_e|}{F_e} \quad (1)$$

where, $RE$ = relative error; $F_s$ = simulated draft force, and $F_e$ = tested draft force.

Table 4 showed that all the relative errors were less than 4%. Accordingly, DEM was proved to be an effective way for simulating the working process of subsoilers. It could be used for predicting the draft force of a newly designed subsoiler accurately without doing the tedious field test, which would save time and energy. Moreover, DEM could avoid some factors in field tests such as the weather, heterogeneity of soil, and other unpredictable conditions which would interfere the

measurement. Therefore, DEM could be applied in optimizing the structure of subsoilers and analyzing their working process.

**Table 4 Simulated draft force and relative errors**

| Subsoiler with points | Simulation/N | Experiment/N | Relative error/% |
|---|---|---|---|
| $T_1$ | 4332 | 4474 | 3.17 |
| $T_2$ | 3001 | 2943 | 1.97 |
| $T_3$ | 3138 | 3022 | 3.84 |
| $T_4$ | 2790 | 2885 | 3.29 |

A subsoiler with wings could increase the disturbance area which will benefit the root grown. However, a pair of wings could increase the draft force as much as 1531 N by analyzing the subsoiler with $T_1$ and $T_2$ only. The geometrical shape of points has affected the subsoilers' draft force significantly by analyzing the data of the subsoiler with $T_2$, $T_3$, and $T_4$. It showed that $T_4$ would cause the minimum draft force and $T_3$ had the largest force among these three points both in the experiment and simulation. The draft force of the subsoiler with $T_2$ was larger than $T_4$ mainly because of the point's complex surface structure. The front face of $T_3$ was much longer than $T_4$ and $T_2$ which meant it disturbed more area and suffered from larger soil resistance. The simulated results reflected the same trend with the experiment in the lab which showed that DEM provided us an effective and accurate way to predict the draft force of subsoilers.

## 4 Other observations

Disturbed area is an index to evaluate the quality of tillage. The particle dynamics could be obtained by slicing the direction of subsoiler traveling. The velocity field of soil particles was observed when the point's tip traveled at the middle of the soil bin (Figure 9). Soil particles were colored by the magnitude of the velocity (Figure 9a). Particles with high velocities were around the subsoiler - soil contacting parts. The disturbed area is shown by screen shots of velocity contours. The side view of $T_1$ and $T_2$ were the same in shape, while $T_1$ has a larger disturbed area because of the pair of wings. The disturbed area of $T_3$ was larger around the points compared with $T_4$, which was caused by the longer edge of $T_3$. The complex shape of the point would increase the draft force while the disturbance areas were almost the same by comparing $T_2$ and $T_4$. Figure 9 also showed that chisel type points could disturb more upper soil particles compared with $T_2$.

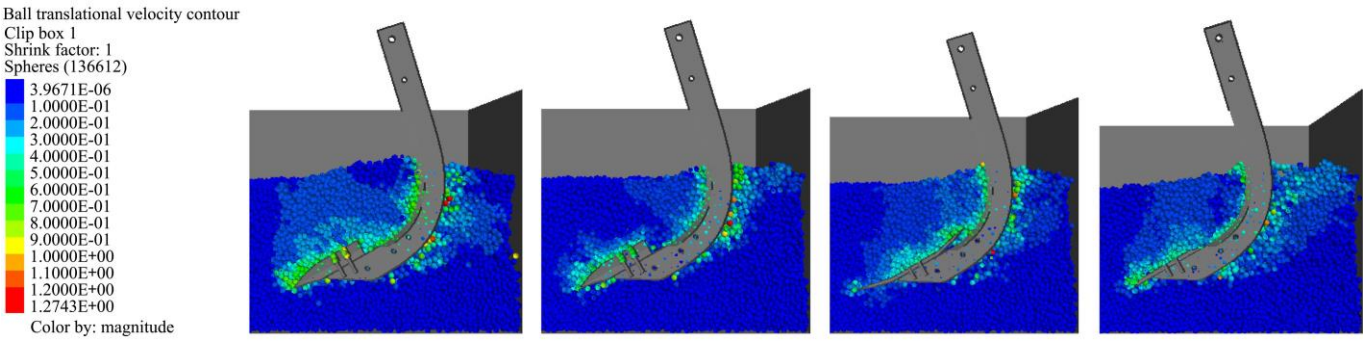


a. The velocity contour, unit is m $s^{-1}$ b. Subsoiler with $T_1$ c. Subsoiler with $T_2$ d. Subsoiler with $T_3$ e. Subsoiler with $T_4$

Figure 9 Screenshots of velocity field

## 5 Conclusions

Four different points were compared in this study both by in-lab experiment and DEM simulation. Soil particle stiffness was calibrated using a standard arc-shaped subsoiler by comparing its simulated draft force with the experiment data. The calibrated particle stiffness was $1.1\times10^4$ N/m. Subsoilers with four different points were then simulated by traveling through the calibrated soil domain. The relative errors of simulated draft force were less than 4% when compared with the experiment results, which shows that DEM is an effective way to predict the draft force. Point's shape has a significant effect on a subsoiler's draft force. It showed that the draft force of the subsoiler with $T_4$ was the least among the four tested; $T_1$ cost the largest draft force mainly because of the pair of wings. Further researches would focus on comparing the tillage performance of points using DEM.

## Acknowledgment

This study was funded by the National Science and Technology Supporting Plan of China (2011BAD29B08).

## [References]

[1] He J, Li H W, Gao H W. Subsoiling effect and economic benefit under conservation tillage mode in Northern China. Transactions of the CSAE, 2006; 22(10): 62–67. (in Chinese with English abstract)

[2] Zhu R, Zhang J, Xue S, Yao W, Li J, Deng H. Experimentation about subsoiling technique for conservation tillage. Transactions of the CSAE, 2009; 25(6): 145–147. (in Chinese with English abstract)

[3] He J, Li H, Wang X, McHugh A D, Li W, Gao H, Kuhn N J. The adoption of annual subsoiling as conservation tillage in dryland maize and wheat cultivation in northern China. Soil & Tillage Research, 2007; 94: 493–502.

[4] Zhang H, Araya K, Kudoh M, Zhang C, Jia H, Liu F, et al. An explosive subsoiler for the improvement of meadow soil, part 1: thermodynamics. J. agric. Engng Res, 2000; 75: 97–105.

[5] Makanga J T, Salokhe V M, Gee-Clough D. Effect of tine rake angle and aspect ratio on soil failure patterns in dry loam soil. Journal of Terramechanics, 1996; 33(5): 233–252.

[6] Luo X, Shao Y, Qiu G, Wen H. The application of soil deep loosening technique in sugarcane production. Transactions of the CSAM, 1997; 28(1): 39–42. (in Chinese with English abstract)

[7] Ahmed M H, Godwin R J. The influence of wing position on subsoiler penetration and soil disturbance. J. agric. Engng Res, 1983, 28: 489–492.

[8] Oni K C, Clark S J, Johnson W H. The effects of design on the draught of undercutter-sweep tillage tools. Soil & Tillage Research, 1992, 22: 117–130.

[9] Shmulevich I, Asaf Z, Rubinstein D. Interaction between soil and a wide cutting blade using the discrete element method. Soil & Tillage Research, 2007; 97: 37–50.

[10] Godwin R J. A review of the effect of implement geometry on soil failure and implement forces. Soil & Tillage Research, 2007; 97: 331–340.

[11] Godwin R J, O'Dogherty M L. Integrated soil tillage force prediction models. Journal of Terramechanics, 2007; 44: 3–14.

[12] Guo Z, Tong J, Zhou Z, Ren L. Review of subsoiling techniques and their applications. Transactions of the CSAE, 2001; 17(6): 169–174. (in Chinese with English abstract)

[13] Mouazen A M, Neményi M. Finite element analysis of subsoiler cutting in non-homogeneous sandy loam soil. Soil & Tillage Research, 1999; 51: 1–15.

[14] Mouazen A M, Neményi M. Tillage tool design by the finite element method: part 1. finiteelement modelling of soil plastic behavior. J. Agric. Engng Res, 1999; 72: 37–51.

[15] Mouazen A M, Neményi M, Schwanghart H, Rempfer M. Tillage tool design by the finite element method: part 2. Experimental validation of the finite element results with soil bin test. J. Agric. Engng Res, 1999; 72: 53–58.

[16] Mouazen A M, Ramon H. A numerical-statistical hybrid modelling scheme for evaluation of draught requirements of a subsoiler cutting a sandy loam soil, as affected by moisture content, bulk density and depth. Soil & Tillage Research, 2002; 63: 155–165.

[17] Mak J, Chen Y, Sadek M A. Determining parameters of a discrete element model for soil–tool interaction. Soil & Tillage Research, 2012, 118: 117–122.

[18] Tamás K., Jóri I J, Mouazen A M. Modelling soil–sweep interaction with discrete element method. Soil & Tillage Research, 2013; 134: 223–231.

[19] Ucgul M, Fielke J M, Saunders C. 3D DEM tillage simulation: Validation of a hysteretic spring (plastic) contact model for a sweep tool operating in a cohesionless soil. Soil & Tillage Research, 2014; 144: 220–227.

[20] Zhang R, Chen B, Li J, Xu S. DEM Simulation of Clod Crushing by Bionic Bulldozing Plate. Journal of Bionic Engineering Suppl. , 2008, 72–78.

[21] Chen Y, Munkholm L J, Nyord T. A discrete element model for soil-sweep interaction in three different soils. Soil & Tillage Research, 2013; 126: 34–41.

[22] Shmulevich I. State of the art modeling of soil–tillage interaction using discrete element method. Soil & Tillage Research, 2010; 111: 41–53.

[23] Itasca, PFC$^{3D}$ particle flow code in three dimensions, theory and background. Itasca Consulting Group, Inc., Minneapolis, MN, USA. 2008.

[24] Sadek M A, Chen Y. Microproperties calibration of discrete element models for soil-tool interaction. ASABE/CSBE Paper No. 1911030. St Joseph, MI, USA: ASABE. 2014.

[25] Li B, Liu F, Xia R, Chen J. Distinct element method analysis and experiment of a biomimetic subsoiler. International Agricultural Engineering Journal, 2015; 24(1): 47–54.

[26] Van der Linde, J., Discrete element modeling of a vibratory subsoiler. MSc Thesis. Department of Mechanical and Mechatronic Engineering, University of Stellenbosch, Matieland, South Africa. 2007.

[27] JB/T 9788-1999. Subsoiler and share shaft. Machinery industry standard of the people's Republic of China. (in Chinese)